The Dissipating Energy Flow method for analysing generator contribution to power system damping

Evaluation and interpretation



Hampus Möller

Division of Industrial Electrical Engineering and Automation Faculty of Engineering, Lund University

Abstract

Electromechanical oscillations is a power system phenomenon where generator rotors oscillate, leading to oscillatory power flows. Damping of such oscillations is important for system stability. Forced oscillations is a special case where one faulty component is the source of the oscillation. This report concerns the Dissipating Energy Flow (DEF), which is an energy-based method for analysing damping performance of individual network components through synchrophasor measurements. It has shown promise in being able to locate the source of a forced oscillation. Through simulations in simple systems the method is evaluated in its ability to 1) locate the source of forced oscillations and 2) indicate the performance of power system stabilisers (PSS). The method succeeds in locating the sources of forced oscillations, while the simulations show no use of the method in indicating PSS performance when the system is disturbed by a forced oscillation. The former is in line with existing literature, but the latter is in conflict with the proposed equivalence between dissipating energy and damping. The results further suggest that the P-f term of the DEF integral alone is responsible for its utility. The simulations indicate that the method's functionality builds on the fact that the source always exhibits a leading phase in an oscillation. This leading phase is demonstrated using data from a real oscillation event. With the help of a mechanical analog the net damping done by the power due to relative rotor angles between machines is analysed, which gives an understanding of the connection between the phase-leading characteristics of the source generator and its dissipating energy flow.

Preface

This thesis finishes my Master's degree in Engineering Physics at the Faculty of Engineering, Lund University. The work has been pursued at the division of Industrial Electrical Engineering and Automation (IEA) in collaboration with Forsmarks Kraftgrupp AB, supervised by Prof. Olof Samuelsson at IEA and Dr. Thomas Smed at Forsmark.

The original idea of the thesis was to use PMU measurement data to study the damping characteristics of the Forsmark nuclear power plant. There was interest in the possible negative interference between nuclear reactor dynamics and oscillations in the power grid, and the generator's PSS settings were believed to be sub-optimal. The Dissipating Energy Flow method was found interesting as a possible way of gaining knowledge about Forsmark's behaviour in relation to power system oscillations; the method seemed to be able to quantitatively assess the damping characteristics of different components of a system in real-time using only PMU data.

The plan was to spend the first month learning about the method and implementing it in Simulink, to confirm its ability to estimate the damping of individual network components, and later apply the algorithm on real PMU data and analyse the damping behaviour of the Forsmark generator. The project however ran into dual obstacles: Firstly, PMU data was not as easily accessible as first assumed. The process of receiving data is still not completed as of writing this. Data provided by local measurements at the Forsmark generator unfortunately proved not to be accurate enough for use with the method.

Secondly, the Simulink implementation of the method showed that the output from the algorithm was very difficult to analyse – the connection between damping performance and dissipating energy flow was not obvious. Simulations were at this point performed in a four-machine system, but the peculiarity of the results called for further simplifications. I went back to the original derivation of the method to find ways of interpreting its output. In the jungle of power system energy functions I was unable to convince myself about the physical relevance of the definition of the dissipating energy flow.

This fact, in combination with the lack of useful data, made me spend my efforts on the understanding of the method itself. Through my Simulink models I was able to closely study the method's behaviour and evaluate its functionality. Evaluation and interpretation of the method then became the subject of the thesis.

The thesis thus ended up in a much more theoretical and academic shape than originally planned. While it lacks any straightforward implementable results, my hope is that it has somehow contributed to the scientific knowledge in its area.

To close up, I want to deeply thank my supervisors for their help in my work. Prof. Olof Samuelsson, for his eternal availability for advice and great enthusiasm about my work, and Dr. Thomas Smed, for his belief in my findings and inspiring personality. I also want to send special thanks to the staff at the IEA division, who kindly let me enjoy almost endless amounts of sandwiches and coffee during the course of this project.

Hampus Möller, 2019-02-01

Contents

1	Intr	oduction	4
	1.1	Objectives	5
2	The	orv	6
_	2.1	Electromechanical oscillations in power systems	6
		2.1.1 The synchronous machine	6
		2.1.2 Two machines	9
		2.1.3 Power system stabilisers	11
	2.2	Dissipating energy flow	11
		2.2.1 Energy in electromechanical oscillations	11
		2.2.2 The DEF integral	12
3	Met	thod & modelling	14
	3.1	Generator model	14
	3.2	Power system models	14
		3.2.1 Single-machine infinite bus	14
		3.2.2 Two-machine system	15
		3.2.3 Simulation settings	15
	3.3	DEF calculation	16
		3.3.1 Input signals	16
		3.3.2 Filtering	16
		3.3.3 Integration	17
		3.3.4 Linear fit	17
		3.3.5 Verification	17
4	Sim	ulations	18
	4.1	Locating forced oscillations	18
		4.1.1 Continuous disturbance	18
		4.1.2 Transient disturbance	21
	4.2	Indicating PSS performance	21
		4.2.1 Single-machine infinite bus	22
		4.2.2 Two-machine system	22
	4.3	Discussion on results	24
		4.3.1 Interpretation as energy	24
5	Rela	ating results to voltage phase angles	27
	5.1	The P - f integral and voltage phase angles	28
	5.2	Phase lead of source generator	30
	5.3	Voltage phase angles in multimachine systems	32
6	Con	clusive discussion	34

7	Future work	35
Α	Model parameters A.1 Generator parameters A.2 Excitation system/AVR parameters A.3 Power system stabiliser	39
в	Further results	41

Chapter 1

Introduction

Phasor Measurement Units (PMUs) are becoming increasingly common in power systems. They provide voltage and current measurements in the form of phasors, which means they provide information about the absolute phase angle of sinusoidal signals. The measurements have high resolution and are synchronised to within 1 μs over continent-wide areas [1], opening the door to new kinds of system operation based on monitoring. Currently the Swedish TSO has 53 PMUs installed [2].

Electromechanical oscillations is a well-known resonance phenomenon in electric power systems. They typically involve two ore more generator rotors oscillating around their equilibrium, leading to oscillatory power flows in their electrical interconnections. For example, two groups of generators situated far apart can oscillate in antiphase with each other, which is known as inter-area oscillations. The oscillations result in fluctuations on all electrical quantities, which reduces the capacity of the system, tears the machines and at worst might result in loss of synchronism, often with an associated blackout. It is stated in a CIGRE report [2] that "The damping of inter-area oscillations is a major concern for many power system operators today."

In recent years it has been investigated how PMU data can be used in relation to electromechanical oscillations [3]. By continuously monitoring the occurrence and behaviour of oscillations, actions could be taken in control rooms to prevent them or mitigate their effects. Control rooms could for example manually change the load flow or the geographical allocation of power generation to alter the resonance, or disconnect a faulty component responsible for an oscillation.

One method for monitoring oscillations that has shown promise is the Dissipation Energy Flow (DEF) method, originally proposed in [4]. It is based on the connection between energy dissipation and damping, which is an established fact in the field of mechanics. In a mechanical oscillation non-conservative forces like friction act to dissipate energy which reduces the amplitude of the oscillation. Analogously, the DEF method uses the rate of oscillatory energy dissipation in a power system as an indicator of damping action. It uses the notion of transient energy from transient stability analysis when referring to the oscillatory energy in a sustained oscillation. The benefits of this method are that it does not rely on models and it can be used in control rooms in a decentralised manner in real-time. It has been shown that the method succeeds in locating the sources of forced oscillations [5]; that is, components that create periodic disturbances affecting the rest of the system. The method has been successfully implemented in ISO-New England as a means of locating forced oscillation sources [6].

Despite its proven ability in this application, the method sometimes shows unexpected behaviour and there is some ambiguity about the physical meaning of the transient energy, as described in the conclusion of [7]. Furthermore, indicating the performance of power system stabilisers (PSS) is a suggested application of the method [8], but its ability in this context has not been rigorously tested. In the light of this, the thesis seeks to establish what the method can be used for and provide improved understanding of the fundamental physics behind it.

1.1 Objectives

With the aim to evaluate the DEF method, the main objectives of this work are to

- 1. Test an implementation of the method in SimPowerSystems (Matlab/Simulink) environment and try its ability to
 - (a) Locate the source of forced oscillations
 - (b) Indicate the performance of power system stabilisers
- 2. Analyse the fundamental physics that make the method work in certain contexts.

Locating oscillation sources and indicating PSS performance are the main suggested applications of the method. As stated earlier the method has already proven its ability to do the former, but this investigation is repeated here with the purposes of replicating the results and gaining understanding of the physics behind it.

Chapter 2

Theory

This chapter starts with an introduction to electromechanical oscillations, which is of fundamental importance for the rest of the report. The second half of the chapter briefly shows the derivation of the DEF method.

2.1 Electromechanical oscillations in power systems

The physical behaviour of power systems is mainly dictated by synchronous machines, which usually constitute most of the generation. As mentioned in the introduction, electromechanical oscillations is a phenomenon where the rotors of synchronous machines oscillate in conjunction with oscillations in their electrical interconnections. They can arise after a transient disturbance, eg. a cleared fault, or as a result of a continuous disturbance by a faulty component. Since the behaviour of electromechanical oscillations is closely connected to the dynamics of synchronous machines, these are introduced below.

2.1.1 The synchronous machine

A synchronous generator is fundamentally a rotating electromagnet (rotor) surrounded by wound conductors that are connected to the grid. The rotor is attached to a rotating energy source (eg. a turbine) whose energy is converted to electrical power. The dynamics of the rotor is governed by the swing equation:

$$2H\frac{\mathrm{d}^2\delta}{\mathrm{d}t^2} = P_m - P_e \tag{2.1}$$

where H is the inertia constant of the machine in per-unit seconds, δ is electrical rotor angle in radians (with respect to synchronously rotating reference), P_m and P_e are the mechanical and electrical powers, respectively, in per-unit.

The mechanical power P_m , coming from the energy source (or prime mover) of the machine, acts to accelerate the rotor. The electrical power output P_e is the power supplied to the grid, which acts to decelerate the rotor.

A block diagram of a generator model is shown in Figure 2.1. The electromagnet in the rotor is energised by the field voltage V_f coming from the excitation system, which usually has an automatic voltage regulator (AVR) to control the voltage at the generator terminals. Additionally a power system stabiliser (PSS) can be installed to enhance the damping characteristics of the generator. The input signal to the excitation system/AVR is the difference between measured terminal voltage V_t and the reference voltage V_{ref} , plus the signal V_{pss} from the PSS.

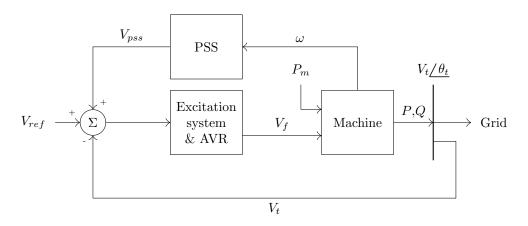


Figure 2.1: A block diagram of a generator connected to the grid.

Classical generator model

A common simplified model of the generator is the so-called classical model, where the generator is modelled as a constant AC voltage source E_q behind a reactance X_d , X'_d or X''_d . This assumes that the excitation (and thus E_q) is constant (i.e. the influence of voltage regulator and power system stabiliser is neglected or assumed zero). The classical model of a generator is shown in Figure 2.2, where the generator is connected to an infinite bus (an ideal voltage source). The complex voltage angle associated with E_q is the electrical rotor angle δ .

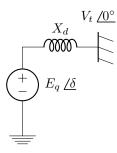


Figure 2.2: A single-machine infinite bus modelled with classical generator model.

The power transmitted through the reactance in Figure 2.2 is

$$P_e = \frac{E_q V_t}{X_d} \sin \delta \tag{2.2}$$

where V_t is the voltage at the infinite bus. Inserting this expression to the swing equation (2.1), we get

$$2H\frac{\mathrm{d}^2\delta}{\mathrm{d}t^2} = P_m - \frac{E_q V_t}{X_d} \sin\delta \tag{2.3}$$

In steady-state, the mechanical and electrical powers P_m and P_e are equal, which means the rotor angle δ is constant. If the system is disturbed, the rotor angle deviates from the steady-state according to the dynamics in the above equation. If the deviation is small enough the system can be linearised around the steady-state values. The deviation in electrical power output is linearised to

$$\Delta P_e = \frac{E_q V_t}{X_d} \cos\left(\delta_0\right) \Delta \delta \tag{2.4}$$

where $\delta = \delta_0 + \Delta \delta$ and δ_0 is the steady-state rotor angle. The dynamic equation for the linearised system becomes

$$2H\frac{\mathrm{d}^2\Delta\delta}{\mathrm{d}t^2} = \Delta P_m - \frac{E_q V_t}{X_d} \cos\left(\delta_0\right) \Delta\delta \tag{2.5}$$

This is a second-order dynamic equation in $\Delta\delta$ that dictates the dynamics of this simple system. The acceleration of the rotor $d^2\Delta\delta/dt^2$ is negatively proportional to the rotor position $\Delta\delta$. This means that when the rotor deviates from its steady-state, it experiences a force that acts to eliminate the deviation. The electrical power in (2.4) thus acts to synchronise the rotor with the rest of the system, which is why it is called synchronising power (very closely related to synchronising torque).

The dynamics of this simple system can be described by means of the mechanical analog shown in Figure 2.3. The dynamic equations of this system are equivalent to those of the generator with the following interpretations (indicated in the figure): The internal voltage E_q corresponds to the length of a bar attached to a flywheel, and its angle is the angle of the bar. The infinite bus is a fixed bar. The electrical power in Eq. 2.2 is represented by the spring force, which is proportional to $\sin(\delta)$. The stiffness of the spring is proportional to the inverse of the internal reactance X_d . The mechanical power on the rotor is represented as a torque T_m acting on the flywheel, which has rotational inertia proportional to H.

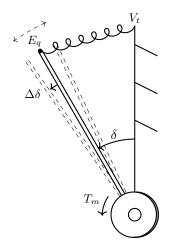


Figure 2.3: A mechanical analog for the single-machine infinite bus system. The radial distance from the joint corresponds to voltage magnitude and angle corresponds to complex voltage angle. The torque T_m represents the mechanical power from the turbine. The flywheel has moment of inertia proportional to H.

If the bar is pushed by an external force, it starts oscillating around the equilibrium: when $\Delta\delta$ is positive the spring force grows, pushing the bar back towards the equilibrium, and when $\Delta\delta$ is negative the mechanical torque T_m is larger than the spring force which also pushes the bar back towards the equilibrium.

This system is conservative so if it is temporarily disturbed it oscillates forever. The energy alternates between the forms of kinetic energy in the flywheel and potential energy in the spring: When $\Delta \delta = 0$ the bar has maximum kinetic energy and no potential energy; when it is on either end point the opposite holds.

As stated earlier, this system is equivalent to the synchronous generator, where energy alternates between kinetic energy in the rotor and electrical potential energy. Such an oscillation is called an electromechanical oscillation since it is an interplay between electrical and mechanical forces acting on the rotor.

Generator model with field circuit dynamics

So far the theory has been based on the classical generator model, assuming constant excitation in the rotor. In reality the field circuit, which is energised by the exciter, has a dynamic behaviour. Since the AVR and PSS directly affect the excitation of the field circuit, the field circuit dynamics play an important role in analysing the impact of AVR and PSS. These dynamics are nonlinear, but assuming small deviations from steady-state they can be linearised. Figure 2.4 shows a block diagram for the linearised behaviour of a machine including the field circuit dynamics, taken from [9]. The electrical output power deviation ΔP_e is proportional to the electrical torque on the rotor $\Delta T_e = K_1 \Delta \delta + K_2 \Delta \Psi_{fd}$. The power can thus be written

$$\Delta P_e = K_1' \Delta \delta + K_2' \Delta \Psi_{fd} \tag{2.6}$$

Here $\Delta \Psi_{fd}$ denotes the field flux linkage (the magnetic flux created by the field circuit). The first term of the expression corresponds to the electrical power in the classical model (Eq. 2.4). The second component in Eq. 2.6 is a novelty of the improved model. It is created by the excitation system and is called the field flux power P_{ff} . This power component can be used to provide improved system damping, which is further discussed in section 2.1.3.

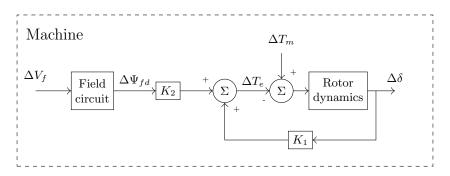


Figure 2.4: A small-signal block diagram of the internal machine model, taken from [9]. All states are represented by deviations from steady-state. V_f denotes field voltage, Ψ_{fd} denotes field flux linkage, T_e is torque due to electrical power output, T_m is mechanical torque and δ is the electrical rotor angle (load angle).

2.1.2 Two machines

Since all generators in power systems are electrically connected, their P_e terms are interdependent. This means that oscillatory modes involving several generators can arise.

Consider a system of two generators, each modelled with the classical generator model, as shown in Figure 2.5. The machines are connected through the reactances X_1 and X_2 , respectively, to a load. In the same way as before, the system can be thought of as a mechanical system, see Figure 2.6. The left picture shows the situation at steady-state, where the mechanical torques T_{m1} and T_{m2} are balanced against the active load P_l .

The right picture shows deviations from steady-state angles in the case of some disturbance, which means the steady-state values are subtracted from each value. Both generators oscillate around the steady-state, which is the vertical line in the figure. The spring forces that represent the electrical power act to push the rotors back towards the steady-state, but the rotational moments of inertia in the rotors keep the oscillation going. Just like the single-machine system this is a conservative oscillation which preserves its oscillatory energy.

This oscillation corresponds to two machines or two groups of machines oscillating ("swinging") against each other in the power system, which is a common type of electromechanical oscillations.

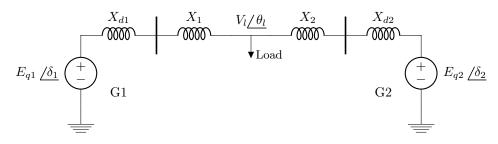


Figure 2.5: A two-machine system modelled with the classical generator model.

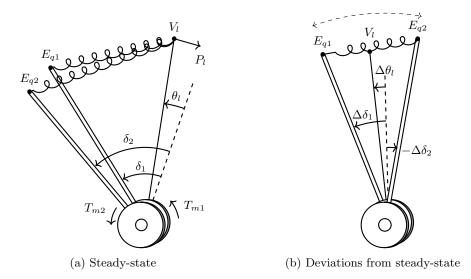


Figure 2.6: A mechanical analog for the two-machine system. The generator bars are connected to flywheels with moment of inertia proportional to H of the two machines respectively. The length of the bars correspond to voltage magnitudes, and their angles correspond to complex voltage angles. The torques T_m represents the mechanical power from the turbine. The load is represented by a bar without moment of inertia. P_l represents the active power drawn by the load.

The term inter-area oscillations, mentioned in the introduction, refers to a situation when the involved machines are far apart.

We now turn to generators modelled according to the linearised model from Figure 2.4. Consider again two generators connected to a load. The electrical power output from one generator can now be written

$$\Delta P_e = K_1' \Delta \delta + K_2' \Delta \Psi_{fd} \tag{2.7}$$

where $\hat{\delta}$ is the difference between electrical rotor angle (δ) and voltage angle at the load (θ_l). This is a generalisation of the original expression from [9] (Eq. 2.6), which was derived in a single-machine infinite bus system. The generalisation is based on recognising the first term in the expression as the output power from the classical model (the spring force from the mechanical analog). In the two-machine case this is proportional to the rotor angle displacement relative to the angle at the load, rather than absolute rotor angle.

Consider the relative load angle deviation $\Delta \hat{\delta}_1 = \Delta \delta_1 - \Delta \theta_l$ in the mechanical analog (Fig. 2.6b). Assuming that the load has no inertia, which means that the angle $\Delta \theta_l$ instantly reacts to any net force it experiences, $\Delta \hat{\delta}_1$ is always proportional to $\Delta \delta_1 - \Delta \delta_2 = \Delta \delta_{12}$. We may therefore write

$$\Delta P_e = K_1'' \Delta \delta_{12} + K_2' \Delta \Psi_{fd} \tag{2.8}$$

with some constant K_1'' . It is important for the later analysis to note that the electrical power has one component proportional to rotor angle separation $\Delta \delta_{12}$.

It should be noted that a different way of expressing the output power is

$$\Delta P_e = K_S \Delta \delta + K_D \Delta \omega \tag{2.9}$$

where ω is the rotor angular velocity. This expression is the traditional division into synchronising and damping power components of the generator output power. The synchronising power is proportional to the local rotor angle δ rather than the relative load angle $\hat{\delta}$. (The term *synchronising* thus refers to synchronisation with respect to a fixed rotating reference, rather than synchronisation with respect to the angle at the load or the mean angle of the system). The expression in (2.8) is not equivalent to the division into damping and synchronising power: Both $K_1''\Delta\delta_{12}$ and $K_2'\Delta\Psi_{fd}$ may contain synchronising and damping components, respectively.

To avoid confusion, $K_1''\Delta\delta_{12}$ will be referred to as the *relative synchronising power* (P_{Srel}) , due to its effect of aligning a generator relative to the rest of the system.

2.1.3 Power system stabilisers

A power system stabiliser is designed to add damping to electromechanical oscillations. This is accomplished by adding an auxiliary signal to the input of the exciter as shown in Figure 2.1. As shown earlier, the output electrical power is

$$\Delta P_e = K_1' \Delta \hat{\delta} + K_2' \Delta \Psi_{fd} \tag{2.10}$$

The second component is used by the PSS to create a damping torque, which fundamentally is any torque that acts in opposite direction of momentary velocity of the rotor. A field flux linkage $\Delta \Psi_{fd}$ that is proportional to rotor speed deviation $\Delta \omega$ creates a component of ΔP_e that is in phase with $\Delta \omega$, which corresponds to a damping torque. The challenge for the PSS is to provide an exciter input signal V_{pss} so that the corresponding field flux $\Delta \Psi_{fd,pss}$ is proportional to $\Delta \omega$. The transfer function from V_{pss} to $\Delta \Psi_{fd,pss}$ mainly consists of a phase lag (delay) that is inherent in the field circuit. To compensate for this delay, V_{pss} should be ahead of (lead) $\Delta \omega$ in phase.

2.2 Dissipating energy flow

We now turn our attention to the method which is the main topic of the thesis, the dissipating energy flow method. As mentioned in the introduction, it builds on the link between energy dissipation and system damping.

2.2.1 Energy in electromechanical oscillations

Electromechanical oscillations behave much like any mechanical oscillation; damping is equivalent to loss of oscillatory energy which reduces the oscillation amplitude. Good system damping thus corresponds to high energy dissipation. Conversely, energy injection corresponds to negative damping or oscillation amplification.

The oscillations can be classified as either natural or forced. The former is what has been discussed so far – a short disturbance that starts some longer lasting motion of the system. In this case energy is injected to the system during the disturbance, and the damping characteristics of the system determines the rate of transient energy dissipation.

In a forced oscillation the system is continuously disturbed by some faulty component that oscillates by itself, which means that energy is continuously injected to the system. This energy must be dissipated somewhere else for the system to remain stable. If the oscillation is stationary, the rate of dissipation is the same as the rate of injection. Normally the rate of dissipation in a system increases when the amplitude of the oscillation increases, which eventually makes the oscillation settle at an equilibrium point of equal dissipation and injection. The better the damping of a system, the more energy injection is needed for a given oscillation amplitude to appear. Most work in this thesis will be spent on forced oscillations, mostly because they create a stationary oscillation which is easy to analyse.

Energy functions in power systems have been used extensively in the field of transient stability analysis where so-called transient energy functions have been used to understand stability issues of post-fault systems. Much effort has gone towards constructing sufficiently accurate energy functions. One way of doing this (which will be referred to later) is presented in [10], where a so-called structure-preserving energy function is derived. Structure-preserving means that the network is not collapsed into an equivalent network consisting of only the internal nodes of the generators; instead, the original structure (topology) of the network is retained in the energy function. The function is constructed starting from Kirchoff's current law, using the fact that the sum of all currents in a node, multiplied by any number, is zero.

$$\int [\boldsymbol{Y}_{\text{bus}} \boldsymbol{V}_{\text{bus}} - \boldsymbol{I}_{\boldsymbol{G}} + \boldsymbol{I}_{\boldsymbol{L}}]^{\mathrm{T}} \mathrm{d} \boldsymbol{V}_{\text{bus}} = 0 \qquad (2.11)$$

Here Y_{bus} is the bus admittance matrix, V_{bus} is the bus voltage matrix, I_G is a vector of currents in all generators and I_L is a vector of currents in all loads. The expression in the square brackets thus corresponds to Kirchoff's current law in all nodes of the network, which must equal zero. The trick is to multiply it by the increment of the bus voltage matrix dV_{bus} and then expand the individual terms. The whole procedure can be found in [11].

2.2.2 The DEF integral

As mentioned above, energy functions have commonly been constructed to reflect the energy injection during a transient disturbance. In [4] the notion of transient energy is expanded to include the oscillatory energy in a sustained oscillation. Inspired by the energy function construction method mentioned above, it is argued that a measure of the oscillatory energy flow from node i to j in a network is

$$\int \operatorname{Im}(\boldsymbol{I_{ij}^*} \mathrm{d}\boldsymbol{V_i}) \tag{2.12}$$

where I_{ij}^* is the complex conjugate of the phasor of current flowing from node *i* to *j*, dV_i is the increment of the voltage phasor at node *i* and Im() denotes the imaginary part. Note that this energy flow is zero when the increment dV_i is zero, i.e. when the complex voltage is constant. The energy flow is present only when the system deviates from its steady-state. Other than that, the physical meaning of the quantity in (2.12) is nontrivial and has no intuitive interpretation. The expression certainly is similar to one term in (2.11), but this expression is never explicitly claimed to be a measure of energy.

It is proven in [11] that the energy flow can be rewritten as

$$\int \operatorname{Im}(\boldsymbol{I_{ij}^*} \mathrm{d}\boldsymbol{V_i}) = \int \left(P_{ij} \mathrm{d}\boldsymbol{\theta}_i + \frac{Q_{ij}}{V_i} \mathrm{d}V_i \right)$$
(2.13)

where P_{ij} and Q_{ij} are active and reactive powers flowing from bus *i* to *j*, respectively, θ_i is the complex voltage angle at node *i* and V_i is the amplitude of the complex voltage. Let $P_{ij} = P_{ij}^0 + \Delta P_{ij}$ and $Q_{ij} = Q_{ij}^0 + \Delta Q_{ij}$, where P_{ij}^0 and Q_{ij}^0 are steady-state equilibrium values. The powers are thus represented by steady-state constants plus deviations from steady-state. We then have

$$\int \left(P_{ij} \mathrm{d}\theta_i + \frac{Q_{ij}}{V_i} \mathrm{d}V_i \right) = \int \left(P_{ij}^0 \mathrm{d}\theta_i + \frac{Q_{ij}^0}{V_i} \mathrm{d}V_i \right) + \int \left(\Delta P_{ij} \mathrm{d}\theta_i + \frac{\Delta Q_{ij}}{V_i} \mathrm{d}V_i \right)$$
(2.14)

In a sustained oscillation the oscillatory energy flows back and forth through different components. Looking at one particular location, the flow constantly changes direction. The energy that flows between different components but is kept within the system is the conservative energy flow, while the energy that is lost to the surrounding is non-conservative. Damping or dissipation of energy corresponds to non-conservative energy flow.

The first integral on the right-hand side of Eq. 2.14 is path-independent, which means it reflects conservative energy. The second integral thus contains all the non-conservative energy, which is the energy dissipation or injection. The second term alone is therefore called the dissipating energy flow:

$$\text{DEF}_{ij}(t) = \int \left(\Delta P_{ij} d\theta_i + \frac{\Delta Q_{ij}}{V_i} dV_i \right) = \int \left(2\pi \Delta P_{ij} \Delta f_i dt + \frac{\Delta Q_{ij}}{V_i} dV_i \right)$$
(2.15)

where $\Delta f_i = \dot{\theta}_i / (2\pi)$ is the local deviation from reference frequency at node *i*. This integral is the quantity that the DEF method is based on. It is interpreted as a measure of energy, which means that its time derivative is the instantaneous flow of energy.

The integral can be computed with PMU measurement data. As usual one has to be careful with signs of currents (and thereby powers). Assuming that it is computed at the terminals of a generator (which is mostly the case in this report), P and Q are positive when power flows from the generator. If the DEF is decreasing, the dissipating energy flow has the opposite sign, i.e. there is a net flow of oscillation energy into the generator. If the DEF is increasing, the generator injects oscillation energy to the system. This is key for interpreting the output of the method.

General interpretation:

- Negative DEF slope = oscillation energy dissipation = damping
- Positive DEF slope = oscillation energy injection = negative damping

It should be noted that in the original version of the method [4], all currents are assumed to be measured out from a node, meaning that generator currents become negative. Therefore, an increasing DEF has the opposite meaning, corresponding to energy flow *into* the generator. However in more recent work on the subject ([5] and [12]), the current from generators are taken to be positive, which is the chosen convention in this report.

Chapter 3

Method & modelling

Simulations are performed in SimPowerSystems in Matlab/Simulink. In order to simplify physical interpretations, the chosen power system models are the simplest possible; single- and two-machine systems. A crucial part of the model is the generator, modelled in the same way throughout all simulations. It is described in detail below. Furthermore, the chosen simulation scenarios and settings are presented as well as the procedure for calculating the DEF.

3.1 Generator model

The generators are modelled using three different blocks in Simulink: Machine, excitation system and PSS (compare to Figure 2.1). The electrical machine is modelled using the *Synchronous machine* block in Simulink, modelling the machine with d- and q-axis equivalent circuits according to model 2.2 in the IEEE standard 1110 [13]. It is a sixth-order model with two equivalent rotor windings on both direct- and quadrature axis, parameterised in the standard way. The parameters of the 187 MVA, 13.8 kV generators are listed in Appendix A.

The excitation system and AVR are modelled together using the Excitation System block in Simulink, implementing a DC exciter as described in IEEE Standard 421.5 [14] and a firstorder voltage regulator. The generators are equipped with power system stabilisers, which are implemented according to IEEE standard PSS1A. The input signal is mechanical rotor angular velocity ω and output is the stabilising voltage signal V_{pss} which is added to the reference voltage to the exciter (see Figure 2.1). Two lead-lag filters are used to produce a forward phase-shift of the signal as explained in section 2.1.3. All the parameters for the excitation system and PSS are found in Appendix A. Since the dynamics of a turbine is slow compared to the phenomena investigated in this report, the mechanical power P_m is assumed to be constant (except for cases when a disturbance is added on P_m).

3.2 Power system models

Two different power system models are used: A single-machine infinite bus model, being the simplest and most understandable power system representation, and a two-machine model being able to reproduce the interaction between two generators.

3.2.1 Single-machine infinite bus

Figure 3.1 shows the single-machine infinite bus (SMIB) system. The reactance X_{line} is 0.6 p.u. (no resistance). The Simulink simulator cannot have the machine, modelled as a current source,

connected directly in series with the inductance, which is solved by adding a small resistive load of 1 MW at the generator terminal.

By applying a transient disturbance and performing Fourier analysis of the induced oscillations the system resonance frequency is determined to be 0.87 Hz.



Figure 3.1: The SMIB system.

3.2.2 Two-machine system

Figure 3.2 shows the two-machine system. The reactances on the lines are $X_1 = 0.6$ p.u. and $X_2 = 0.3$ p.u. (no resistances). The system is intentionally chosen to not be completely symmetric, since a disturbance in the middle of a symmetric system would not excite the resonance mode. The machines are operated at close to nominal power, and the load is modelled as constant impedance (drawing 370 MW and 100 MVar). By applying a transient disturbance and performing Fourier analysis of the induced oscillations the system resonance frequency is determined to be 1.02 Hz. The two-machine model implementation in Simulink is shown in Figure 3.3.

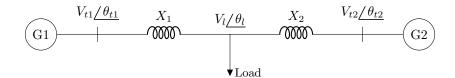


Figure 3.2: The two-machine system.

3.2.3 Simulation settings

The system is simulated for 30 seconds, which is 15 periods of the slowest oscillation and should be enough to get accurate results. Some different solvers and time steps are tried for solving the system, and they are compared to see which ones offer sufficient accuracy. The system is simulated using phasor simulation, which means that all impedances are evaluated at the fundamental frequency and currents and voltages in all nodes are represented as complex numbers. This simplifies the system of differential equations which results in faster solving. The results are validated against a normal time-domain simulation where all differential equations are solved explicitly. The chosen solver is the ode3 in Simulink, which is a third-order-of-accuracy solver using the Bogacki-Shampine integration technique. It uses a fixed time step and to be able to accurately model the voltage angle dynamics a short time step of 10^{-4} s is used.

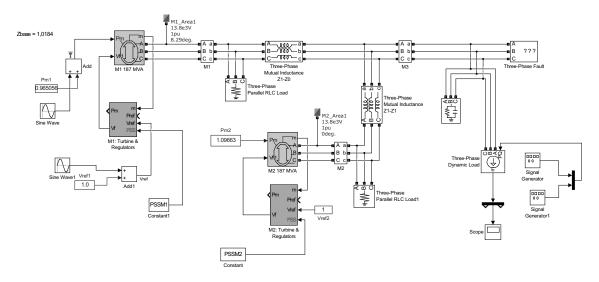


Figure 3.3: The Simulink implementation of the two-machine system. The *Sine Wave* and *Signal Generator* blocks are the disturbance sources.

3.3 DEF calculation

The DEF integral is evaluated at the terminals of each generator. The *Three-Phase V-I Measurement* block in Simulink is used to measure complex voltages and currents, corresponding to PMU measurements. These signals are sent to the Matlab workspace where the DEF algorithm is executed after the simulation. An overview of the algorithm is shown in Figure 3.4.

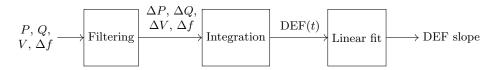


Figure 3.4: An overview of the DEF algorithm.

3.3.1 Input signals

The input signals to the calculation are active power P_{ij} , reactive power Q_{ij} , voltage magnitude V_i and local frequency deviation Δf_i (see Eq. 2.15). These are simply obtained from the complex voltages and currents (local frequency deviation is the derivative of complex voltage angle). The signals are down-sampled by a factor of 100 for quicker processing, meaning the effective sampling frequency in the processing step is 100 Hz.

3.3.2 Filtering

The first step is to compute the deviations from steady-state values of the input signals, as they appear in the DEF formula (2.15). As suggested in [5], this is accomplished by bandpass filtering the signals with a pass band around the frequency of the mode in question. This removes steady-state values and also any fluctuations not participating in the mode. Filtering is done with the Matlab functions fdesign.bandpass (designing a filter to meet specific criteria) and filtfilt (performing forward-backward filtering, which preserves the phase of the filtered signals).

The filters are designed to have cutoff frequencies $0.7f_0$ and $1.3f_0$ where f_0 is the pass frequency. For all forced oscillation cases, the stopband attenuation is set to 15 dB, allowed passband ripple to 1 dB and filter order to 500. The frequency response of all used filters are visually examined to ensure sufficient filter quality. To lower the requirements for the bandpass filter, linear trends are removed from the signals before filtering (using Matlab function detrend). To remove the distortion effects in the ends of the filtered signals, 500 samples (17% of the data sequence) are removed from the beginning and the end of all signals, respectively. Since any remaining constant offset of the filtered signals is detrimental to the DEF computation, the mean of the final signals are subtracted (even though this should not be necessary considering the bandpass filter).

3.3.3 Integration

The DEF integral is calculated by a summation over all time steps, corresponding to the forward Euler rule. For convenience the voltage magnitude V_i in (2.15) is replaced by the mean voltage magnitude over the interval. This should not affect the result much since only a small part of V_i varies. The explicit numerical formula then becomes

$$\text{DEF}_{ij,t+1} = \text{DEF}_{ij,t} + 2\pi\Delta P_{ij,t}\Delta f_{ij,t}\tau + \Delta Q_{ij}\frac{\Delta V_{i,t+1} - \Delta V_{i,t-1}}{2\overline{V_i}}$$
(3.1)

where τ denotes the sample time and $\overline{V_i}$ is the mean voltage magnitude. Δ -variables correspond to the filtered signals. The terms $2\pi\Delta P_{ij,t}\Delta f_{ij,t}\tau$ (*P*-*f*-term) and $(\Delta Q_{ij}\Delta V_{i,t+1} - \Delta V_{i,t-1})/2\overline{V_i}$ (*Q*-d*U*-term) are also summed separately.

3.3.4 Linear fit

The slope of the DEF integral corresponds to the rate of energy dissipation. This is the key quantity in the method since it is an indicator of damping performance. In each simulation a least-squares straight line fit to the DEF function is computed from which the slope is extracted. The value of the slope, which is the output from the algorithm, thus reflects the mean derivative of the DEF integral.

3.3.5 Verification

The implementation of the algorithm is verified using the test case library developed in [15]. Simulation data from different cases of natural and forced oscillations are downloaded and the DEF computation algorithm is run on this data. The results are consistent with the results in [5]: The DEF slope indicates the location of the oscillation source. This verifies the implementation of the algorithm.

Chapter 4

Simulations

In this chapter all simulation scenarios are described and the results are shown and discussed. The results are divided with respect to the two applications of the method: Locating the source of forced oscillations and indicating PSS performance.

4.1 Locating forced oscillations

The dissipating energy flow can be used to locate the source of forced oscillations since the source is the component that injects oscillatory energy to the system. In this application the DEF slope is interpreted as follows:

Positive DEF slope = oscillation energy injection = source of forced oscillation

The two-machine system is used to evaluate the method's ability in this context. In the first section, the system is continuously disturbed by a sinusoidal disturbance added to either the mechanical power P_m or the exciter reference voltage V_{ref} of generator 1. The former corresponds to a faulty turbine, governor or frequency controller; the latter to a faulty exciter, AVR or PSS. In the second section the system is transiently disturbed by a short-circuit, and the PSS is tuned to be negative in generator 1, which corresponds to a malfunctioning PSS. All cases create a sustained oscillation in which generator 1 is the oscillation source.

4.1.1 Continuous disturbance

Sinusoidal disturbances with 0.05 p.u. amplitude are added to either P_m or V_{ref} of generator 1. The frequency of the disturbance is varied to cover a range of frequencies both below and above the resonance frequency of the system, with focus on frequencies close to resonance.

For each simulation the DEF slope is calculated according to the procedure introduced in the previous chapter, which is visualised in Figure 4.1. It shows the DEF computation process for generator 1 in simulation F5a, where the disturbance frequency coincides with the resonance frequency. The input signals P, Q, V and Δf are first bandpass filtered and then sent to the DEF algorithm. A linear fit is computed for the resulting graph and from this the slope is extracted.

Figure 4.2 shows the DEF at both machines during the same simulation. It is clear that the DEF is increasing at generator 1 and decreasing at generator 2.

A list of all continuous disturbance simulations and the resulting DEF slopes are shown in Table 4.1. In all simulated cases the DEF slope at generator 1, which is the source of the oscillation, is positive while the slope at generator 2 is negative. This means that the DEF method works for oscillation source identification in all the simulated cases, just as it has shown to do before [5].

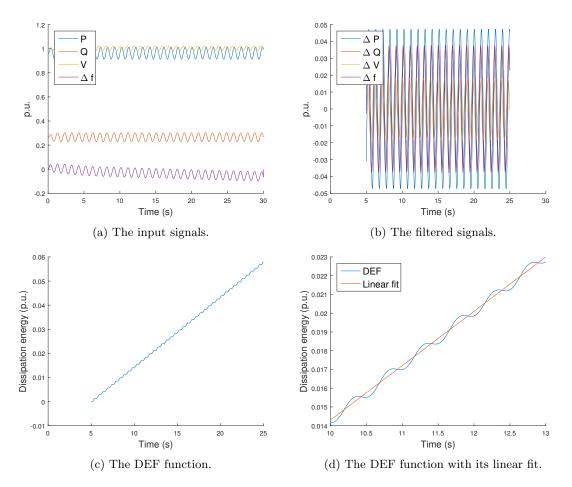


Figure 4.1: The process of computing the DEF slope in simulation F5a at generator 1.

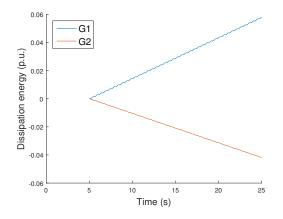


Figure 4.2: The DEF at both generators in simulation F5a. The slopes are 2.9 p.u./1000 s and -2.1 p.u./1000 s, respectively.

Simulation ID	Disturbance	G1 DEF slope	G2 DEF slope	Comment
		p.u./1000 s	p.u./1000 s	
F1a	$P_m \ 0.5 \ \mathrm{Hz}$	3.672	-0.525	
F1b	$P_m \ 0.5 \ \mathrm{Hz}$	1.953	-0.133	Without PSS
F2	$P_m 0.75 \text{ Hz}$	4.988	-2.691	
F3	$P_m 0.9 \text{ Hz}$	4.329	-3.227	
F4	$P_m 0.99 \text{ Hz}$	3.436	-2.550	
F5a	P_m 1.02 Hz	2.899	-2.095	
F5b	P_m 1.02 Hz	11.650	-13.680	Without PSS
F6	P_m 1.05 Hz	2.754	-1.935	
F7	P_m 1.1 Hz	2.649	-1.773	
F8	P_m 1.5 Hz	1.580	-0.903	
F9	$P_m \ 2 \ \mathrm{Hz}$	0.607	-0.425	
F10	$V_{ref} 0.5 \text{ Hz}$	0.346	-0.046	
F11	V_{ref} 0.9 Hz	0.411	-0.183	
F12a	V_{ref} 1.02 Hz	0.185	-0.088	
F12b	V_{ref} 1.02 Hz	2.285	-1.341	Without PSS
F13	V_{ref} 1.1 Hz	0.120	-0.059	
F14	V_{ref} 1.5 Hz	0.028	-0.014	
F15	$V_{ref} \ 2 \ \mathrm{Hz}$	0.011	-0.004	

Table 4.1: All results from forced oscillation source identification. Generator 1 is always the source of the oscillation. The system resonance frequency is at 1.02 Hz.

4.1.2 Transient disturbance

In this section the system is disturbed by a three-phase short-circuit at the load, lasting for 100 ms. The PSS on generator 1 has negative gain, which produces negative damping and creates a sustained oscillation in which generator 1 is the oscillation source.

Figure 4.3 shows the result of this simulation. After the transient disturbance a sustained oscillation is created as seen in the left picture. The right picture shows the DEF at both machines. It clearly shows that G1 is the generator with negative damping, since its DEF is increasing. The DEF slopes thus manages to locate the source of the oscillation.

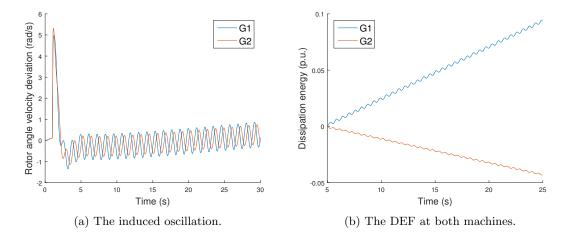


Figure 4.3: A simulation of a natural oscillation in the two-machine system, induced by a shortcircuit disturbance. The PSS on generator 1 has negative gain.

4.2 Indicating PSS performance

The second application of the method concerns the PSS performance of generators. Since the rate of energy dissipation is equivalent to damping, the DEF slopes of different machines should be able to reveal their relative contribution to system damping. This application builds on the following DEF interpretation:

More negative DEF slope = higher oscillation energy dissipation = more damping

To evaluate the method's ability to indicate PSS performance, the slopes of the DEF integrals are compared and related to varying PSS settings. Simulations are done in both the single-machine infinite bus and the two-machine system.

For most cases the system is continuously disturbed by a constant-amplitude disturbance because this creates a stationary disturbed operation which is easy to analyse. The drawback of using this disturbance is that the rate of energy injection depends on the response of the system. A constant-amplitude disturbance creates a steady-state where injected and dissipated energies are the same. When the PSS settings are varied, the overall damping of the system changes, which means the steady-state point changes. For a given disturbance amplitude the rate of energy injection changes according to an interplay between the disturbance motion and the system motion. Therefore a change of steady-state point means a possible change in disturbance energy injection. Some care should be taken when comparing the absolute DEF slopes between different simulations; they are manifestations of the equilibrium energy injection/dissipation and not necessarily proportional to damping performance. The simulation scenarios are designed to overcome this difficulty.

4.2.1 Single-machine infinite bus

In the SMIB system a disturbance is introduced on the voltage angle on the infinite bus, which is set to oscillate sinusoidally. The amplitude of the disturbance is chosen so that the rotor oscillation is the same in comparable simulations (simulations with the same disturbance frequency), which means that the oscillation energy is kept the same. This means the DEF slopes can be compared between simulations at the same frequency.

Table 4.2 shows the results from these simulations. A larger disturbance amplitude, inducing the same rotor oscillation, corresponds to better damping. An example is simulations S3a and S3b in the table, where S3a has a significantly smaller disturbance amplitude while keeping roughly the same rotor oscillation amplitude, meaning that the PSS provides damping. It is clear that the PSS acts to dampen the oscillation when the frequency is close to resonance (S2-S4), but it has no effect when the frequency is far from resonance (S1 and S5). In the latter cases the system is well-damped in itself so it makes sense for the PSS to not help.

In all simulations the DEF slope is significantly more negative when the PSS is turned on. In close-to-resonance cases (S2-S4) this is expected. The improved damping means more energy is injected (the disturbance amplitude is increased), and consequently more energy is dissipated.

Problematically though, the DEF slope decreases also in cases S1 and S5, when the PSS does not actually provide damping. Both the disturbance amplitude and rotor oscillation stay the same after the PSS is introduced, so we expect the energy dissipation in the generator to also stay the same, but it dramatically decreases just as in cases S2-S4. This might suggest that the DEF slope indicates whether or not the PSS is turned on, rather than the actual damping it provides.

Simulation ID	Frequency	PSS	$A_{\rm dist}$	A_{δ}	DEF slope
	Hz		Degrees	Degrees	p.u./1000 s
S1a	0.5	Off	2	3.3	0.005
S1b	0.5	On	2	3.7	-0.224
S2a	0.8	Off	0.6	4.6	-0.406
S2b	0.8	On	2	5.2	-5.061
S3a	0.87	Off	0.3	3.7	-0.557
S3b	0.87	On	2	4.1	-4.774
S4a	1.0	Off	0.8	2.2	-0.472
S4b	1.0	On	2	2.5	-3.671
S5a	1.5	Off	2	1.0	-0.975
S5b	1.5	On	2	1.0	-3.571

Table 4.2: Results from simulations to indicate PSS settings in SMIB system. A_{δ} is amplitude of rotor oscillation, A_{dist} is amplitude of disturbance. The resonance frequency is 0.87 Hz.

4.2.2 Two-machine system

Let us now turn to the two-machine system. Here we hope to be able to tell the relative contributions of the machines to the overall system damping. A continuous disturbance is introduced as a varying load, corresponding to a few percent of the total load. In half of the scenarios the active power is fluctuating, in the rest the reactive power is fluctuating.

As mentioned above, the absolute DEF slopes are hard to understand during constant-amplitude disturbances since the energy input from the disturbance source is unknown and may vary between scenarios. In this section we thus only attempt to compare the DEF slopes of the two machines within each simulation scenario, and relate this to their PSS settings. This is a realistic application of the method: monitoring the DEF flows in different generators to identify good and bad damping performance from different PSS implementations.

The disturbance frequencies are chosen in a similar manner as above, taking into account the resonance frequency of the respective systems. For each frequency four different scenarios are simulated:

- Both: Both generators have PSS
- G1 on: Only generator G1 has PSS
- G2 on: Only generator G2 has PSS
- None: None of the generators has PSS

The complete results can be found in Appendix B, and a summary of the results is visualised in Figure 4.4. It shows the DEF slope for each machine at different disturbance frequencies, divided into groups corresponding to different PSS settings. The slopes are expected to show the relative damping contribution of each machine. When the PSS is turned on in one of the machines, its DEF slope is expected to generally become more negative (assuming that the PSS works and provides damping). For example, the DEF slope in scenario "G1 on" is expected to be more negative at generator 1 than at generator 2, since generator 1 contributes more to system damping.

This is however not the case in the simulated scenarios; the distribution of slopes seem to be roughly the same for both machines independent of PSS setting. At the same time the simulations clearly show that the PSS generally does improve the damping of the system when it is turned on (see Appendix B). This means that the method fails to indicate the relative damping contribution of each machine. In other words, looking only at the DEF slope of the two machines in any single simulation, it is impossible to tell which of the machines has active PSS.

The sum of the slopes, which should reflect total damping from both generators, also behaves a bit strangely. The sum is sometimes positive, which would suggest that the generators provide negative damping. Negative damping from the generators during a forced oscillation seems like something that would make the system unstable, but it seems well-damped in all cases. Perhaps damping comes from other components in the system (eg. the load), which is discussed later.

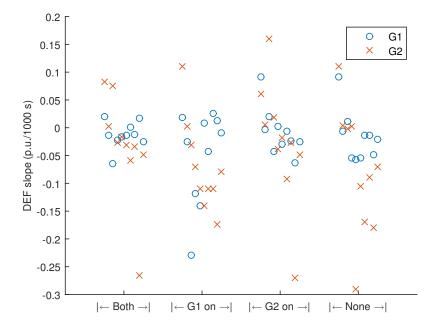


Figure 4.4: A summary of the results for indicating PSS performance in a two-machine system with continuous disturbance. The shown data corresponds to DEF slopes in simulations S6-S10 and SQ6-SQ10 (complete results found in Appendix B). They are grouped with respect to the four different PSS setting scenarios.

4.3 Discussion on results

The results of the evaluation are mixed. They clearly confirm the method's ability to locate the source of forced oscillations. This holds for all three simulated disturbance sources: disturbance on mechanical power, disturbance on voltage regulator reference and negative PSS gain following a transient disturbance.

The results concerning PSS performance are worse. In the SMIB system the DEF seems to show whether the PSS is turned on rather than the actual damping it provides. The method fails to distinguish which machine has active PSS in the forced oscillation in the two-machine system. This is a proposed application of the method [8] which seems impracticable within the boundaries of this investigation.

4.3.1 Interpretation as energy

The inherent interpretation of the DEF function as a flow of energy deserves some attention. The starting-point expression $\int \text{Im}(I_{ij}^* dU_i)$ is derived rather heuristically, and as stated in [7]: "(...) the physical meaning of the transient energy (...) is still not clear even after decades of study." In this section the simulated results are analysed with respect to this issue.

Energy balance

In a sustained oscillation the energy flow into the system should equal the energy flow out from the system. In the two-machine system case, the sum of dissipating energy flows from both generators should equal the dissipating energy flow into the load (of course the energy must not have this direction; it may flow from the load to the generators, which would result in negative signs).

An example of this is shown in Figure 4.5, which shows the dissipating energy flow from simulation F5a. Energy flows from generator 1, which is the source of the disturbance, to generator 2 and the load which dissipate energy. Table 4.3 shows the energy balance in some further simulations. Perfect energy balance would mean that each row in the table would add up to zero. The results show that the balance is generally not perfect but acceptable.

The dissipating energy flow into loads has been a reason for concern [3]. Resistive loads may appear as either sources or sinks of dissipating energy [7]. It is strange that a resistance, being a passive element, can appear as a source of energy. This can be seen in simulation F5b in Table 4.3, where the load appears as a source of dissipating energy. The fact that the method is derived using lossless network and constant-power loads might explain this strange behaviour [5].

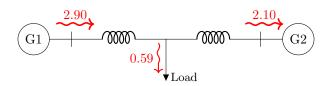


Figure 4.5: The flow of dissipating energy in simulation F5a, in p.u./1000 s. Generator 1 injects dissipating energy and generator 2 together with the load dissipates energy. There is reasonable nodal balance.

Simulation ID	G1 DEF slope	G2 DEF slope	Load DEF slope
	p.u./1000 s	p.u./1000 s	p.u./1000 s
F1a	3.672	-0.525	-3.083
F1b	1.953	-0.133	-1.776
F5a	2.899	-2.095	-0.593
F5b	11.650	-13.884	5.717
F14	0.028	-0.014	-0.007
S6a	0.091	0.112	-0.208
S7a	0.012	-0.002	-0.001
S7c	0.020	0.163	-0.178
S8a	-0.057	-0.288	0.397
S8e	-0.016	-0.016	0.033

Table 4.3: The DEF slopes from chosen simulations in the two-machine system, including the DEF at the load to show nodal balance. The energy flow direction in the load is chosen analogously to the generators: positive DEF corresponds to injection of energy to the system.

Generator dissipation

As stated earlier, the relative flow of dissipating energy in different generators does not seem to be consistent with their relative damping contributions. Furthermore the sum of the DEF slopes in some cases behaves strangely: As a measure of the flow of dissipation energy in both machines combined, it should be a measure of overall damping provided by the generators. When there is a disturbance on the load and the generators provide damping, we expect oscillation energy to flow from the load to the generators. There are however cases in Figure 4.4 (or the tables in Appendix B) where the sum of the generator DEF slopes is positive, meaning that oscillation energy flows from the generators to the load. It appears as if the disturbance comes from the generators and is damped by the load, while in reality it is the opposite.

These observations may suggest that the DEF is not a proper measure of oscillatory energy. On the other hand, generator damping might not necessarily consist of local energy dissipation. Perhaps a generator could contribute to damping by controlling the electrical flows in such a way that much energy is dissipated by another component, for example a load? The actual contribution of a generator to system damping would then not be proportional to the energy dissipated in that particular generator, but rather the amount of energy dissipated as a result of the generator's actions. In that case the DEF might be a valid measure of energy, but still not be able to quantify generator damping contribution.

Chapter 5

Relating results to voltage phase angles

The concept of oscillatory energy can be used to explain some of the results in the previous chapter, especially the method's ability to locate the source of a forced oscillation. But since the physical meaning of the energy flow is unclear, a different explanation to the functioning of the method might be helpful. Such an explanation is developed in this chapter. It focuses on the method's ability to locate the source of forced oscillations, which is its clearest merit.

In understanding the behaviour of the DEF, it is helpful to consider the two terms of the function separately. For convenience the DEF function is repeated here

$$\text{DEF} = \int \left(2\pi \Delta P_{ij} \Delta f_i \text{d}t + \frac{\Delta Q_{ij}}{U_i} \text{d}U_i \right)$$
(5.1)

The first term is referred to as the P-f term, the second as the Q-dU term. As we shall see, these terms do not always behave in the same way.

The DEF slopes from some of the cases F1-F17 are reviewed in Table 5.1, divided into the separate terms. The terms do not always have the same sign. The P-f term always has the same sign as the total DEF, while the sign of the Q-dU term seems uncorrelated. Since the P-f term is usually larger, it seems to generally dictate the behaviour. It appears as if the method would work using only the P-f term; the Q-dU term seems oblivious to where the oscillation source is.

Simulation ID	G1 DEF	G1 <i>P</i> - <i>f</i>	G1 Q -dU	G2 DEF	G2 $P-f$	$G2 \ Q-dU$
	p.u./1000 s	p.u./1000 s	p.u./1000 s	p.u./1000 s	p.u./1000 s	p.u./1000 s
F1a	3.672	3.714	-0.042	-0.525	-0.478	-0.047
F1b	1.953	1.876	0.077	-0.133	-0.163	0.031
F3	4.329	6.263	-1.934	-3.227	-2.292	-0.935
F5a	2.899	4.318	-1.419	-2.095	-1.390	-0.705
F5b	11.650	13.476	-1.826	-13.680	-13.884	0.204
F8	1.580	1.953	-0.373	-0.903	-0.555	-0.349
F10	0.346	0.409	-0.062	-0.046	-0.36	0.315
F12a	0.185	0.096	0.088	-0.088	-0.120	0.031
F12b	2.285	0.995	1.290	-1.341	-1.539	0.198
F14	0.028	0.010	0.018	-0.014	-0.007	-0.007

Table 5.1: The DEF slopes in chosen simulations, showing the separate terms of the DEF.

5.1 The *P*-*f* integral and voltage phase angles

The fundamental functioning of the method thus seems to lie in the *P*-*f* term. Its sign reveals the location of the oscillation source. The DEF is calculated at the generator terminals, so *P* is the generator output power and *f* is the local frequency (the derivative of voltage angle). In a sustained oscillation ΔP and Δf both oscillate around zero. It is the relative phases of these oscillations that determine the sign of the integral $\int 2\pi\Delta P\Delta f dt$. If they are completely in phase, the product is always positive, if they are 180° out of phase, the product is always negative. If they are more in phase than out of phase, that is their absolute phase difference is less than 90°, then the integrand will on average be positive, meaning the integral will increase with time. The opposite happens if their absolute phase difference is more than 90°.

 ΔP and Δf can be represented by phasors (with respect to the oscillation frequency), as shown in Figure 5.1. The shaded area in the figure corresponds to the region where ΔP has an absolute phase difference of less than 90° with respect to Δf . Since Δf is the time derivative of voltage angle at the generator terminals $(\Delta \theta_t)$, The phase of $\Delta \theta_t$ is always 90° behind the phase of Δf as shown in the figure. This means that if the absolute phase difference between ΔP and Δf is less than 90°, ΔP must lead $\Delta \theta_t$ (i.e. there is a phase delay from ΔP to $\Delta \theta_t$ of 0-180°). The following therefore holds:

Lemma 5.1 The P-f integral increases if and only if ΔP leads $\Delta \theta_t$.

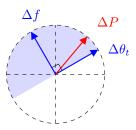


Figure 5.1: Frequency and active power deviations from steady-state, represented as phasors. The shaded region corresponds to being more in phase than out of phase with Δf . If ΔP is in this region, the *P*-*f*-integral will increase with time.

This equivalence is illustrated in Figure 5.2, taken from simulation F5a. For generator 1, ΔP leads $\Delta \theta_t$ which means the *P*-*f* term is increasing, while the opposite is true for generator 2.

As introduced in the theory section, the linearised electrical power output from a generator has two components

$$\Delta P_e = K_1'' \Delta \delta_{12} + K_2' \Delta \Psi_{fd} \tag{5.2}$$

The first term is the relative synchronising power P_{Srel} which is equivalent to the spring force in the mechanical analog, and normally constitutes the major part of the electrical power. Since this term is proportional to $\Delta \delta_{12}$, the behaviour of this angle separation is interesting. For this the following holds:

Lemma 5.2 If $\Delta \delta_1$ leads $\Delta \delta_2$, then the difference $\Delta \delta_{12}$ leads both of them. Conversely, if $\Delta \delta_1$ lags $\Delta \delta_2$, then the difference $\Delta \delta_{12}$ lags both of them.

This equivalence is visualised in Figure 5.3. It means that if generator 1 leads generator 2, then the relative synchronising power P_{Srel} leads the rotor of generator 1.

This has implications for the *P*-*f* integral. Figure 5.4 shows how the deviations of voltage phase angles at different positions in the system typically look. The phase of the voltage angle deviation at the machine terminals $\Delta \theta_t$ is usually somewhere between the phase of the rotor and the phase of the rest of the system. This means that if P_{Srel} leads $\Delta \delta_1$, then it also leads $\Delta \theta_{t1}$. This implies the following

Lemma 5.3 If $\Delta \delta_1$ leads $\Delta \delta_2$, then the relative synchronising power P_{Srel} acting on rotor 1 leads the terminal voltage angle $\Delta \theta_{t1}$. The relative synchronising power therefore contributes with a component to the P-f integral which is increasing. Conversely, if $\Delta \delta_1$ lags $\Delta \delta_2$, then the relative synchronising power lags the terminal voltage angle $\Delta \theta_{t1}$, which contributes to a decreasing P-f integral.

So only the fact that one generator leads the other one in the oscillation implies that the P-f integral grows at this generator, due to the dependence of output power on angle separation. The sign of the P-f integral can thus be thought of as an indicator on which machine leads in the oscillation.

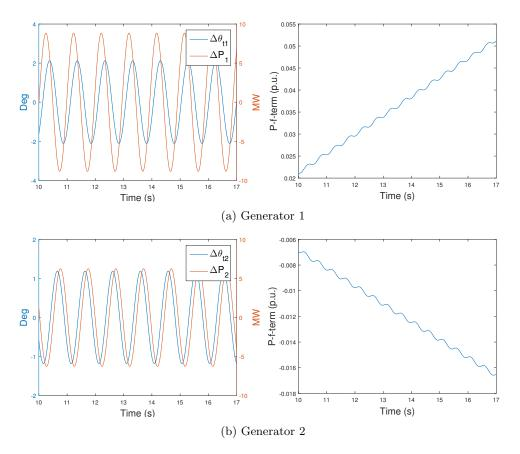


Figure 5.2: An illustration of the relation between the P-f term and the phases of ΔP and $\Delta \theta$. For generator 1, ΔP leads $\Delta \theta_t$ and the DEF increases. For generator 2, ΔP lags $\Delta \theta_t$ and the DEF decreases. Taken from the F5a simulation.

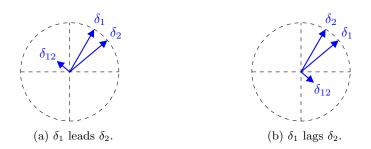


Figure 5.3: A visualisation of Lemma 5.2.

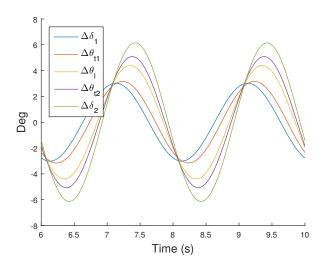


Figure 5.4: Voltage phase angle deviations at different positions in the two-machine system during simulation F1a.

5.2 Phase lead of source generator

In the previous section it was argued that the P-f term indicates which generator leads the oscillation. The remaining question is how this relates to damping.

We turn again to the mechanical analog of the two-machine system from Figure 2.6. The relative synchronising power P_{Srel} is equivalent to the spring force, being proportional to the difference between the rotor angles $\Delta \delta_{12}$. In one time instant this force may act either in opposite direction of the rotor velocity, which means it is a damping force, or in line with the velocity, which is an amplifying force.

In an undamped resonance case, when the rotors oscillate in perfect antiphase, the damping and amplifying forces during an oscillation period are the same, which means that there is no net damping or amplification. This is shown in Figure 5.5, where the relative synchronising power is visualised as arrows proportional to the difference between the rotor angles. The coloured areas indicate the size of the total damping and amplifying forces, respectively, during the whole interval. It is clear that the damping and amplifying forces are the same.

In Figure 5.6, which is taken from the F5a simulation, the rotors do not oscillate in perfect antiphase. Generator 1 can be said to lead the oscillation, although the difference is close to 180°, which makes the "lead" and "lag" terminology a bit confusing. The point is that generator 1 is 0-180° ahead of generator 2. This phase relationship means that the net damping and amplifying forces during a period are not equal.

For rotor 1 the damping force in a period is larger than the amplifying force. The relative synchronising power thus provides damping on rotor 1. The opposite holds for rotor 2, which experiences a net amplifying force during an oscillation period. Any damping that is provided on rotor 1 corresponds to an equal amplification on rotor 2.

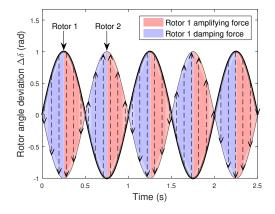


Figure 5.5: The damping and amplifying forces due to relative synchronising power, experienced by rotor 1, when the rotors oscillate in perfect antiphase. The arrows correspond to the instantaneous force, which is proportional to the angle separation, and the coloured areas indicate the size of the total damping and amplifying forces, respectively.

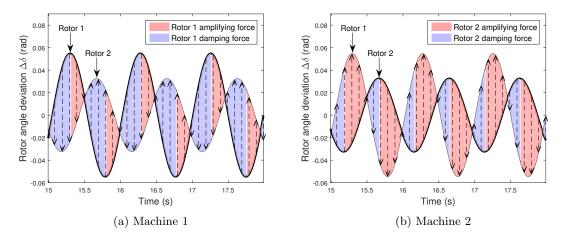


Figure 5.6: The damping and amplifying forces due to relative synchronising power during simulation F5a (forced oscillation on generator 1). The arrows correspond to the instantaneous force, and the coloured areas indicate the size of the total damping and amplifying forces, respectively.

The delay from machine 1 to machine 2 can be thought of as a measure of the net amount of oscillation energy that is transferred between the machines through their rotor angle oscillations. The closer the delay is to 90° , the more oscillatory energy machine 2 takes from machine 1.

This means that the leading generator always experiences net damping from the other generator. It therefore makes sense that the generator that is the source of the oscillation always leads; this way it gets a net damping force from the system.

It can be thought of in terms of steady-state force equilibrium: If a sinusoidal steady-state is reached it means that the net forces on both machines during an oscillation period must be zero. Consider a forced oscillation on generator 1, and assume that the PSS is turned on in generator 2. In generator 1 the rotor experiences a force that is the source of the oscillation. Since rotor 2 lags rotor 1, the relative synchronising torque provides damping on rotor 1, which compensates so that the net force is zero. As described above this damping corresponds to an equal amplifying force on rotor 2. The PSS in generator 2 then creates a damping field flux torque component on rotor 2 which compensates for this amplifying force. The result is that both generators are in sinusoidal steady-state.

Looking at the simulated scenarios, the source generator always leads the oscillation. The amount of damping provided by the other generator seems related to the phase difference. An example is shown in Figure 5.7, taken from simulation F5. When the PSS is turned off, there is almost 180° phase difference. When the PSS is turned on, the phase lag of generator 2 decreases to significantly less than 180°, which results in increased damping on generator 1.

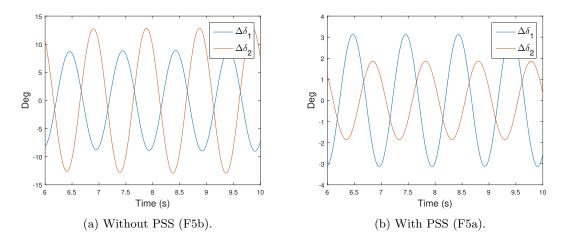


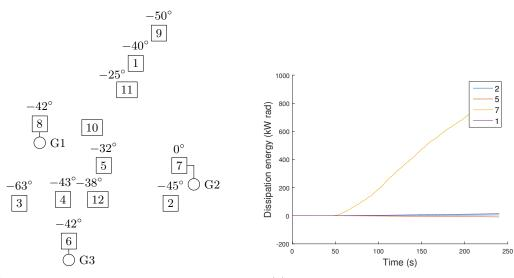
Figure 5.7: The rotor oscillations in simulations F5a-b. When the PSS is turned on, the phase lag from rotor 1 to rotor 2 is closer to 90 degrees.

5.3 Voltage phase angles in multimachine systems

The above argumentation is done with respect to the two-machine system. It is however generalisable to cases with more machines. The relative synchronising power in this case acts to push each rotor towards the mean position of the other rotors. The same concept then applies to one machine's phase relative to all other machines: If one machine leads the oscillation, then it experiences net damping from the rest of the system. In a forced oscillation, the source machine experiences damping from the rest of the system, and so it must lead.

This behaviour can be shown using a real oscillation case from the test case library mentioned earlier [15]. Case 5 is chosen which consists of PMU measurements during a disturbance on January 29, 2018 in New England, where a 1.57 Hz oscillation occurs. The phase angle of the voltage at each bus is analysed: first bandpass filtered for the mode of interest and then transformed with a one-point discrete Fourier transform, to receive the magnitude and phase of the dominant oscillation.

The phase delay at each bus is shown in Figure 5.8a, which builds on an approximate geographical outline of the system. The source of the oscillation in this case is known to be a generator at bus 7. It can be seen that the phase delay generally gets larger further away from the source. This applies to all substations except substation 2 which is surprisingly delayed; perhaps the electrical distance from substation 7 to substation 2 is not as short as suggested by the geographic distance indicated in the picture. The fact that the source generator leads the oscillation is however clear



(a) The approximate geographical location of the substations, represented by boxes with bus numbers, and their phase delays in the oscillation as extracted directly from the PMU data.

(b) The dissipating energy flow through chosen substations, indicated by numbers in the legend.

Figure 5.8: Data from real test case 5 in the test case library [15]. The system oscillates at 1.57 Hz due to a disturbance coming form generator 2 at bus 7.

and gives real-life evidence that this is a general behaviour.

Figure 5.8b shows the dissipating energy flow at some of the substations. It is clear from the figure that the source is at substation 7, which means the method succeeds in locating the source of a forced oscillation in this real-life case.

Chapter 6

Conclusive discussion

The results in this report point towards the following general performance of the DEF method:

- It manages to accurately locate the source of a sustained oscillation, whether it is a mechanical disturbance, disturbance on reference voltage or faulty PSS equipment. It is the P-f term of the DEF expression that provides this behaviour, so the method would work without the Q-dU term.
- It does not manage to tell the damping contribution by a generator during an external disturbance.

These conclusions are based on simulations in small systems and specific operating conditions. It is of course possible that different simulation scenarios may produce different results. One possible reason for the results to underestimate the method performance is the fact that the load is modelled as a constant impedance, while the derivation of the method makes the assumption of constantpower loads. As mentioned before, resistive loads may appear as sources of dissipating energy, which can hardly be explained. There is a possibility that a constant-power load model would produce simulation results where the damping contribution from generators can be obtained from the DEF. Still in that case, the fact that the method fails when the load has constant impedance is of major concern.

Another threat to the validity of the results is that almost all scenarios deal with constantamplitude disturbances. As mentioned above, this is due to the fact that they create sustained oscillations that are easy to analyse. The relation between energy dissipation and damping during these disturbances is however complicated. As described in section 4.2, the amount of energy injected by a constant-amplitude disturbance can vary and is hard to estimate. Perhaps a more realistic type of disturbance is one that injects constant energy rather than has constant amplitude.

The previous chapter suggests that the relative phases of voltage phase angle deviations in a system are key for the method's functionality. The source generator is shown to always lead in the oscillation, and a leading generator automatically gets an increasing DEF integral. The former is not a new finding; a similar reasoning is for instance given in [2] (section 4.4.2.3). This report has contributed with a connection between the phase lead property and the increasing DEF integral. This connection can explain how the method works without relying on energy expressions whose physical meaning is unclear.

Chapter 7

Future work

To enhance the credibility of the results presented in this report, further simulations can be done which 1) do not contain any resistive elements and 2) do not use constant-amplitude disturbances.

The results do neither validate nor dismiss the interpretation of the DEF integral as a real energy flow. It would be interesting to investigate this further, for example: Does the total energy dissipation rate correspond to the rate of decay in the oscillation after a transient disturbance?

The results in this report suggest that the method would work equally well with only the P-f term. This could be tried on different cases of simulated and real data to see if the results remain the same.

Furthermore, since the source of an oscillation can be found by only looking at the relative phases of the oscillation throughout the network, like in Figure 5.8a, perhaps the DEF integral is unnecessary; performing Fourier transforms of the voltage angle deviations might be enough. If one mode is highly dominant a one-point Fourier transform can be used, but perhaps more interestingly, a full Fourier transform can reveal the relative phases of oscillations at all frequencies. In a control room the transform can be computed in real-time, showing the magnitude of all present oscillations along with their relative phases. The oscillation source can be identified based on the fact that it always leads the oscillation.

This is however complicated by the fact that one machine always leads – whether or not the oscillation is forced. In the case of a natural oscillation, perhaps occurring as a result of an overloaded network, the leading generator should not be identified as an oscillation source, which might happen looking only at its relative phase. Perhaps cases of forced oscillations can be distinguished by the size of the phase difference, which might be larger in forced oscillations. Also, the argumentation in this thesis indicates that the leading generator always has a negative damping effect on the rest of the system, meaning that it can be useful to identify the leading machine although it is not a proper oscillation source. This is an interesting area for further research.

As discussed in section 5.2, the dynamics of the rotor can be understood by means of accelerating and damping forces. Just as in ordinary mechanics, one could define the work done by a force as the force times the displacement. Damping and amplifying forces would thus do positive and negative work on the rotor, respectively. In the two-machine case, the work done by the relative synchronising torque is proportional to the integral of angular difference $\Delta \delta_{12}$ times angular velocity deviation $\Delta \omega$. In a similar manner, one could probably find an expression for the work done by the field flux torque. The total work would be the sum of these terms. Then one should be able to see a clear connection between energy and oscillation amplitude: if there is a net negative work on the rotor during an oscillation period, the oscillation amplitude should decrease. This could be built upon to find more intuitive energy expressions for the rotor, which could be used eg. to optimise PSS settings.

Finally, the relation between the DEF method and traditional modal analysis for small-signal

stability could be investigated. In particular, the connection between the real part of an eigenvalue and the corresponding dissipating energy flow is an interesting topic.

Bibliography

- Farrokh Aminifar, Mahmud Fotuhi-Firuzabad, Amir Safdarian, Ali Davoudi, and Mohammad Shahidehpour. Synchrophasor measurement technology in power systems: panorama and state-of-the-art. *IEEE Access*, 2:1607–1628, 2015.
- [2] CIGRE working group C2: Power system operation and control. Wide area monitoring systems support for control room applications. Technical report, CIGRE, 2018. Reference: 750.
- [3] Bin Wang and Kai Sun. Location methods of oscillation sources in power systems: a survey. Journal of Modern Power Systems and Clean Energy, 5(2):151–159, 2017.
- [4] Lei Chen, Yong Min, and Wei Hu. An energy-based method for location of power system oscillation source. *IEEE Transactions on Power Systems*, 28(3):828–836, 2013.
- [5] Slava Maslennikov, Bin Wang, and Eugene Litvinov. Dissipating energy flow method for locating the source of sustained oscillations. *Electrical Power & Energy Systems*, 88:55–62, 2017.
- [6] Samuel Chevalier, Petr Vorobev, Konstantin Turitsyn, Bin Wang, and Slava Maslennikov. Using passivity theory to interpret the dissipating energy flow method, 2018. arXiv:1811.03260v2.
- [7] Lei Chen, Fei Xu, Yong Min, Maohai Wang, and Wei Hu. Transient energy dissipation of resistances and its effect on power system damping. *Electrical Power and Energy Systems*, 91:201–208, 2017.
- [8] Lei Chen, Yong Min, Yi-Ping Chen, and Wei Hu. Evaluation of generator damping using oscillation energy dissipation and the connection with modal analysis. *IEEE Transactions on Power Systems*, 29(3):1393–1402, 2014.
- [9] Prabha Kundur. Power System Stability and Control. EPRI Power System Engineering Series. McGraw-Hill, Inc, 1994.
- [10] Young-Hyun Moon, Byoung-Hoon Cho, Yong-Hoon Lee, and Hyo-Sik Hong. Energy conservation law and its application for the direct method of power system stability. In *IEEE Power Engineering Society*. 1999 Winter Meeting, volume 1, pages 695–700, 1999.
- [11] Young-Hyun Moon, E.-H. Lee, and T.-H. Roh. Development of an energy function reflecting the transfer conductances for direct stability analysis in power systems. *IEEE Proceedings – Generation, Transmission & Distribution*, 144(5):503–509, September 1997.
- [12] Ruichao Xie and Daniel J. Trudnowski. Tracking the damping contribution of a power system component under ambient conditions. *IEEE Transactions on Power Systems*, 33(1):1116– 1117, January 2018.
- [13] IEEE-SA Standards Board. IEEE std 1110: IEEE guide for synchronous generator modeling practices and applications in power system stability analyses. Technical report, IEEE Power Engineering Society, 2002.

- [14] IEEE-SA Standards Board. IEEE std 421.5: IEEE recommended practice for excitation system models for power system stability studies. Technical report, IEEE Power Engineering Society, 2016.
- [15] Slava Maslennikov, Bin Wang, Qiang Zhang, Feng Ma, Xiaochuan Luo, Kai Sun, and Eugene Litvinov. A test cases library for methods locating the sources of sustained oscillations. In *IEEE Power and Energy Society General Meeting*, Boston, MA, USA, 2016.

Appendix A

Model parameters

A.1 Generator parameters

The generator is modelled as a salient pole machine with one pair of poles. General quantities are shown in Table A.1.

Туре	Salient pole
Nominal power	187 MVA
Nominal voltage	13.8 kV (l-l)
Frequency	50 Hz
Number of pole pairs	1

Table A.1: General generator quantities.

The generator parameters, shown in Table A.2, are taken from the example generator in Table 2 at page 39 in the IEEE standard 1110 [13].

Description	Parameter	Unit	Value
d-axis synchronous reactance	X_d	pu	1.3
q-axis transient reactance	X'_d	pu	0.3
d-axis sub-transient reactance	X_d''	pu	0.25
q-axis synchronous reactance	X_q	pu	0.5
q-axis sub-transient reactance	X_q''	pu	0.25
Leakage reactance	X_l	pu	0.2
d-axis transient time constant	T'_d	s	1
d-axis sub-transient time constant	$T_d^{\prime\prime}$	s	0.05
q-axis sub-transient time constant	$T_{qo}^{''}$	s	0.1
Armature resistance	R_a	pu	0.0025
Inertia coefficient	Н	s	4
Friction factor	F	pu	0

Table A.2: Generator parameters.

A.2 Excitation system/AVR parameters

The excitation system plus AVR is modelled using the *Excitation System* block in Simulink, implementing a DC1C excitation system from the IEEE Standard 421.5 [14] (Annex H.2). The

parameters are shown in Table A.3.

Description	Parameter	Unit	Value
Low-pass filter time constant	T_r	s	0.02
Regulator gain	K_a		46
Regulator time constant	T_a	s	0.06
Exciter gain	K_e		1
Exciter time constant	T_E	s	0.46
Transient gain reduction denominator time constant	T_b	s	0
Transient gain reduction numerator time constant	T_c	s	0
Damping filter gain	K_f		0.1
Damping filter time constant	T_{f}	s	1
Regulator output lower limit	$E_{f,min}$	pu	0
Regulator output upper limit	$E_{f,max}$	pu	10

Table A.3: Excitation system parameters.

A.3 Power system stabiliser

The PSS is implemented in Simulink and consists of a sensor, gain, a wash-out high-pass filter, two lead-lag filters and an output limiter, according to IEEE standard PSS1A (Annex H.3 in [14]). The nominal parameters are shown in Table A.4.

Description	Parameter	Unit	Value
Sensor time constant	T_s	s	0
Gain	K		3
Wash-out time constant	T_W	s	10
Lead-lag $\#1$ numerator time constant	$T_{1,n}$	s	0.76
Lead-lag $\#1$ denominator time constant	$T_{1,d}$	s	0.01
Lead-lag $#2$ numerator time constant	$T_{2,n}$	s	76
Lead-lag $#2$ denominator time constant	$T_{2,d}$	s	0.01
Output lower limit	$V_{S,min}$	pu	-0.15
Output higher limit	$V_{S,max}$	pu	0.15

Table A.4: Nominal PSS parameters.

Appendix B

Further results

All results from section 4.2.2 are shown below. They are divided into two tables: Table B.1 where the disturbance is on active load power, and Table B.2 where the disturbance is on reactive load power.

Simulation ID	Frequency	G1 DEF	$A_{\delta G1}$	G2 DEF	$A_{\delta G2}$	Comment
	Hz	p.u./1000 s	Degrees	p.u./1000 s	Degrees	
S6a	0.5	0.091	1.2	0.11	1.1	No PSS
S6b	0.5	0.018	0.9	0.11	0.6	PSS G1
S6c	0.5	0.091	1.0	0.061	0.8	PSS G2
S6d	0.5	0.020	0.8	0.083	0.5	PSS on both
S7a	0.9	0.011	0.6	-0.0019	1.0	No PSS
S7b	0.9	-0.23	0.4	-0.031	1.0	PSS G1
S7c	0.9	0.020	0.7	0.16	0.6	PSS G2
S7d	0.9	-0.064	0.3	0.076	0.3	PSS on both
S7e	0.9	3.0	5.7	-3.0	4.9	PSS G1 negative
S8a	1.02	-0.057	0.9	-0.29	1.5	No PSS
S8b	1.02	-0.14	0.3	-0.11	0.8	PSS G1
S8d	1.02	0.0034	0.4	-0.038	0.3	PSS G2
S8e	1.02	-0.016	0.2	-0.016	0.3	PSS on both
S8f	1.02	3.7	4.7	-1.9	3.6	PSS G1 negative
S9a	1.1	-0.014	0.5	-0.17	0.8	No PSS
S9b	1.1	-0.042	0.2	-0.11	0.6	PSS G1
S9c	1.1	-0.0061	0.3	-0.092	0.3	PSS G2
S9d	1.1	0.001	0.2	-0.059	0.2	PSS on both
S9e	1.1	2.0	3.6	-1.1	2.9	PSS G1 negative
S10a	1.5	-0.049	0.1	-0.180	0.2	No PSS
S10b	1.5	0.013	0.1	-0.174	0.2	PSS G1
S10c	1.5	-0.063	0.1	-0.270	0.2	PSS G2
S10d	1.5	0.017	0.1	-0.266	0.2	PSS on both

Table B.1: All results from simulations in the two-machine system with disturbance on the active power drawn by the load. $A_{\delta G1}$ and $A_{\delta G2}$ are the amplitude of the rotor oscillations in the machines respectively. * means PSS with increased gain.

Simulation ID	Frequency	G1 DEF	$A_{\delta G1}$	G2 DEF	$A_{\delta G2}$	Comment
	Hz	p.u./1000 s	Degrees	p.u./1000 s	Degrees	
SQ6a	0.5	-0.006	2.5	0.004	2.2	No PSS
SQ6b	0.5	-0.025	1.8	0.003	1.4	PSS G1
SQ6c	0.5	-0.003	1.8	0.005	1.7	PSS G2
SQ6d	0.5	-0.014	1.4	0.003	1.1	PSS on both
SQ7a	0.9	-0.055	1.1	0.003	0.3	No PSS
SQ7b	0.9	-0.118	0.9	-0.071	1.5	PSS G1
SQ7c	0.9	-0.043	1.0	0.018	0.2	PSS G2
SQ7d	0.9	-0.022	0.5	-0.026	0.5	PSS on both
SQ7e	0.9	5.105	6.5	-2.685	4.9	PSS G1 negative
SQ8a	1.02	-0.055	0.7	-0.106	1.2	No PSS
SQ8b	1.02	0.009	0.3	-0.14	1.4	PSS G1
SQ8c	1.02	0.043	0.2	-0.160	1.5	PSS G1*
SQ8d	1.02	-0.029	0.6	-0.018	0.3	PSS G2
SQ8e	1.02	-0.013	0.3	-0.031	0.5	PSS on both
SQ8f	1.02	4.177	4.9	-1.960	3.8	PSS G1 negative
SQ9a	1.1	-0.013	0.3	-0.089	0.9	No PSS
SQ9b	1.1	0.026	0.1	-0.110	1.0	PSS G1
SQ9c	1.1	-0.024	0.4	-0.027	0.3	PSS G2
SQ9d	1.1	-0.012	0.2	-0.034	0.4	PSS on both
SQ9e	1.1	2.483	4.0	-1.186	3.2	PSS G1 negative
SQ10a	1.5	-0.021	0.2	-0.071	0.3	No PSS
SQ10b	1.5	-0.009	0.2	-0.079	0.3	PSS G1
SQ10c	1.5	-0.025	0.2	-0.049	0.2	PSS G2
SQ10d	1.5	-0.025	0.2	-0.049	0.2	PSS on both

Table B.2: All results from simulations in the two-machine system with disturbance on the reactive power drawn by the load. $A_{\delta G1}$ and $A_{\delta G2}$ are the amplitude of the rotor oscillations in the machines respectively. * means PSS with increased gain.